Inorganic Chemistry

pubs.acs.org/IC Article

Mechanistic Studies of Alkyne Hydroboration by a Well-Defined Iron Pincer Complex: Direct Comparison of Metal-Hydride and Metal-Boryl Reactivity

Ana L. Narro, Hadi D. Arman, and Zachary J. Tonzetich*



Cite This: Inorg. Chem. 2022, 61, 10477–10485



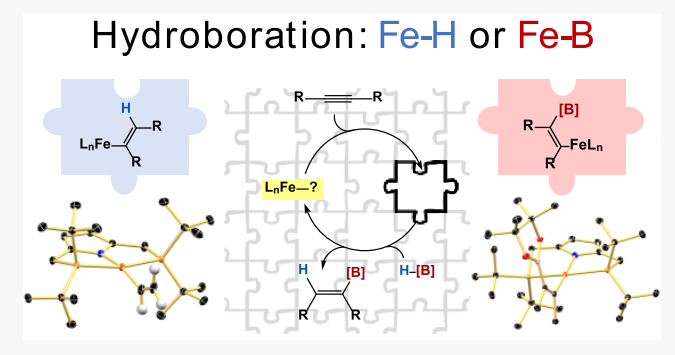
ACCESS I

Metrics & More

Article Recommendations

Supporting Information

ABSTRACT: Iron-hydride and iron-boryl complexes supported by a pyrrole-based pincer ligand, ^{tBu}PNP (PNP = anion of 2,5-bis(di-tert-butylphosphinomethyl)pyrrole), were employed for a detailed mechanistic study on the hydroboration of internal alkynes. Several novel complexes were isolated and fully characterized, including iron-vinyl and iron-boryl species, which represent likely intermediates in the catalytic hydroboration pathway. In addition, the products of alkyne insertion into the Fe–B bond have been isolated and structurally characterized. Mechanistic studies of the hydroboration reaction favor a pathway involving an active iron-hydride species, [FeH(fBuPNP)], which readily inserts alkyne and undergoes subsequent reaction with



hydroborane to generate product. The iron-boryl species, $[Fe(BR_2)(^{tBu}PNP)]$ ($R_2 = pin$ or cat), was found to be chemically competent, although its use in catalysis entailed an induction period whereby the iron-hydride species was generated. Stoichiometric reactions and kinetic experiments were performed to paint a fuller picture of the mechanism of alkyne hydroboration, including pathways for catalyst deactivation and the influence of substrate bulk on catalytic efficacy.

■ INTRODUCTION

Methodologies for the synthesis of vinyl boronic esters have been widely examined through both metal and non-metal-mediated reactions. These compounds tend to be stable for storage and are easy to isolate with high purity. Vinyl boronic esters are desirable synthons as they can be further employed in key transformations, such as coupling partners in Suzuki–Miyaura cross-coupling reactions. The use of transition metal catalysts allows for specific selectivity of potential chemo-, regio-, and enantioselective hydroboration products. Precious metals, mainly rhodium and iridium, have been found to catalyze the hydroboration of unsaturated bonds in excellent yields under mild conditions and with good tolerance for functional groups.

Despite the success of precious metal catalysts, first-row transition metals have garnered great interest in hydrofunctionalization reactions as they offer a potentially more sustainable alternative. Pincer-type ligands, in particular, have been exploited to great effect to design such catalysts as these platforms provide kinetic stability along with electronic and structural versatility. The use of a stable and tunable ligand is key when studying mechanisms of 3d transition metal catalysts as these systems can react through single-electron transfer (SET) pathways, adopt multiple spin states, and have various energetically accessible oxidation states. Among first-row transition metals, iron has become increasingly popular as a

catalyst for hydrofunctionalization reactions due to its natural abundance, low cost, and low toxicity. $^{9-11}$

In the past few years, several groups have reported on the catalytic hydroboration of different substrates using welldefined iron catalysts. 12-20 Thomas and co-workers reported the iron-catalyzed hydroboration of alkenes and alkynes with high functional group tolerance, along with chemo-, regio-, and stereoselectivity.²¹ Kirchner et al. reported a nonclassical iron(II) polyhydride pincer complex.²² Their work highlighted high selectivity toward the corresponding Z-vinylboronates. No mechanism was proposed, but based on the reactivity and selectivity displayed by the metal complex, they suggested the strong likelihood of vinylidene intermediates. The following year, Kirchner and co-workers reported a series of iron(II) bis(acetylide) complexes with reactivity toward hydroalkynylation and hydroboration reactions.²³ Through experimental results and DFT calculations, the active species was reported to be the bis(acetylide) complex, which functioned through a novel mechanism involving a sigma bond metathesis with the

Received: April 19, 2022 Published: June 29, 2022





acetylide ligand, followed by hydride insertion. Webster and co-workers also published an active iron(II) species for the hydroboration of alkenes and alkynes with reactivity toward a wide variety of substrates.²⁴ They proposed a pathway where an iron-hydride complex serves as the key intermediate (Scheme 1).

Scheme 1. Catalytic Cycles for Alkyne Hydroboration

$$R = R$$

$$L_{n}M = R$$

$$R = R$$

$$R$$

Of direct relevance to the current work, Nishibayashi and co-workers reported the selective hydroboration of terminal alkynes catalyzed by an iron(II) system containing the pyrrolebased pincer ligand, tBuPNP (PNP = anion of 2,5-bis(di-tertbutylphosphinomethyl)pyrrole).²⁵ In their report, they suggested the possibility of the active species being an ironhydride complex based on the work presented by Webster et al. However, when they probed a novel iron-boryl complex for catalysis, it was found to have comparable reactivity to the iron-hydride. Mechanisms for catalytic alkyne hydroboration involving both iron-hydride and iron-boryl species can be readily envisioned, as depicted in Scheme 1. Many prior studies have favored a M-H cycle, although the possibility of generating metal-boryl species is rarely considered. The ability of the (tBuPNP)Fe system to readily stabilize both Fe-H and Fe-B species drew our attention, as we have recently demonstrated the ability of iron species other than hydrides to serve as active catalysts in hydrofunctionalization reactions.²⁶

Herein, we report detailed mechanistic studies into the hydroboration of internal alkynes using the iron(II) hydride and boryl complexes displayed in Chart 1. The reactivity of

Chart 1. Iron-boryl and iron-hydride of tBuPNP

both species was studied to scrutinize how their mechanistic pathways relate to one another. By focusing on internal alkynes, we sought to extend the methodology reported by Nishibayashi and potentially avoid any pitfalls arising from the acidity of the acetylene proton.²⁵ In addition, we have been

able to isolate and characterize several key intermediates along the catalytic pathway.

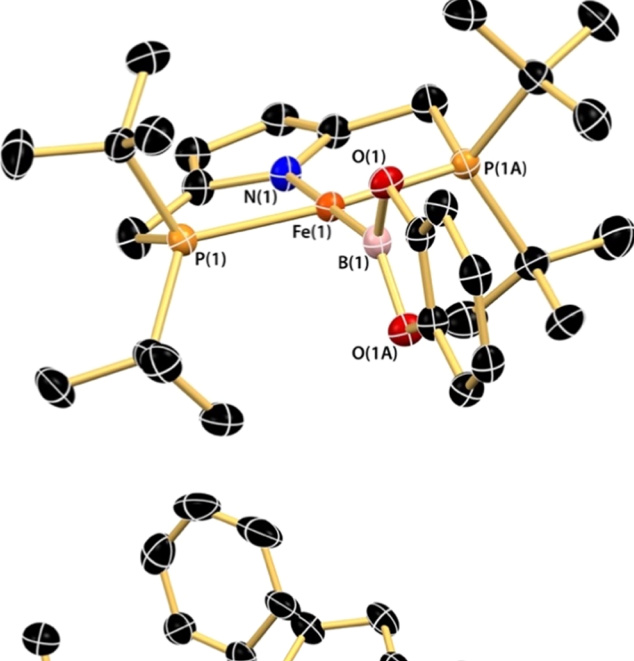
RESULTS

Precatalyst Syntheses. We began our studies by exploring alternative synthetic routes for both the iron-boryl (1a) and the iron-hydride complexes (2) shown in Chart 1. The reported method for the synthesis of 1a involves treatment of 2 with either pinacolborane or bis(pinacolato)diboron, both resulting in suboptimal yields (Scheme 2).²⁵ We have now

Scheme 2. Synthetic Routes to Compounds 1 and 2

identified two new routes for the synthesis of 1a. The first involves oxidative borylation of iron(I) via the treatment of [Fe^I(N₂)(tBuPNP)]²⁷ with bis(pinacolato)diboron. The reaction was found to produce detectable quantities of the desired iron-boryl 1a, but the compound proved difficult to purify. The second route, which is the preferable means of preparing 1a, involves the reaction of a novel iron-bis-phenolate complex (3) with diborane. This method leverages the thermodynamic stability of the resulting PhOBpin byproduct as a way of driving the reaction.²⁸ Complex 3 itself is a high-spin fourcoordinate species with one dissociated phosphine arm. The structure of 3, depicted in Figure 1, exists as a coordination polymer in the solid state with sodium cations forming bridges to the π system of adjacent pyrrolide units (see the Supporting Information). Upon treatment with pinacoldiborane, 3 generates 1a with concomitant reassociation of the phosphine donor. This method was further successful in generating the catecholatoboron species, [Fe(Bcat)(fBuPNP)] (1b). The solid-state structure of 1b also appears in Figure 1 and is essentially identical to that of 1a published previously.²

In addition to 1a and 1b, a related boron-containing complex, $[Fe(BH_4)(^{fBu}PNP)]$ (4), was also prepared and examined as a precursor to iron-hydride 2 (Scheme 2). Borohydride compound 4 is analogous to that previously



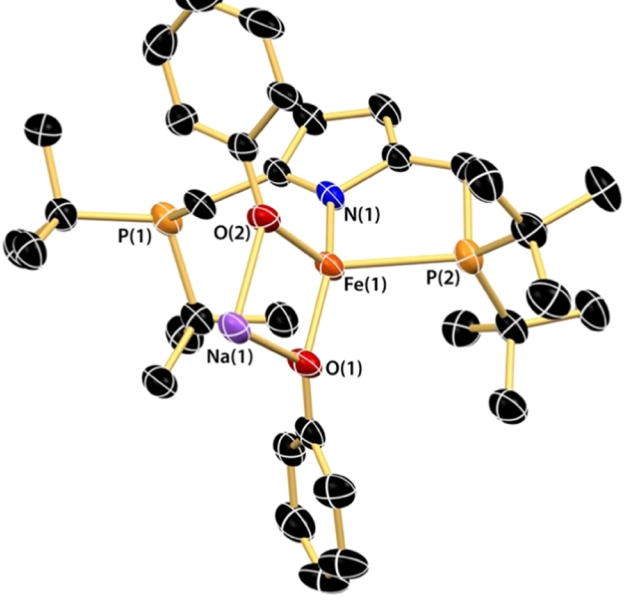


Figure 1. Top: solid-state structure of compound **1b**; bottom: solid-state structure of the molecular unit of **3**. Hydrogen atoms are omitted for clarity. See the Supporting Information for bond distances and angles.

published by our group containing the cyclohexyl-substituted PNP ligand and isostructural to the cobalt analog (see the Supporting Information for the structure of 4). 29,30 In contrast to the $^{\text{CyPNP}}$ variant, however, attempts to generate 2 from 4 through both heating and treatment with phosphine to capture extruded BH_3 proved unsuccessful.

Stoichiometric Reactivity. To gain insight into the mechanism of iron-catalyzed alkyne hydroboration, we first targeted key steps in the cycles displayed in Scheme 1. Complex 1a was treated with different internal alkynes to test for insertion into the Fe–B bond (Scheme 3). Reactions of 1a with 2-butyne and 4-octyne proceeded rapidly at room temperature to afford insertion products 5 and 6 as isolable complexes. ¹H NMR spectra of both compounds display two resonances for the phosphine ¹Bu groups in line with the expected decrease in symmetry from $C_{2\nu}$ to C_S . The pinacol unit appears as a single peak, indicating free rotation about the B–C bond on the NMR timescale (see the Supporting Information). Crystallization of 5 from heptane afforded

Scheme 3. Reactivity of 1a with Internal Alkynes

1a + R

thf

$$R = Me$$
 $R = Me$
 R

crystals suitable for X-ray diffraction. The structure is depicted in Figure 2. The compound retains the square-planar geometry

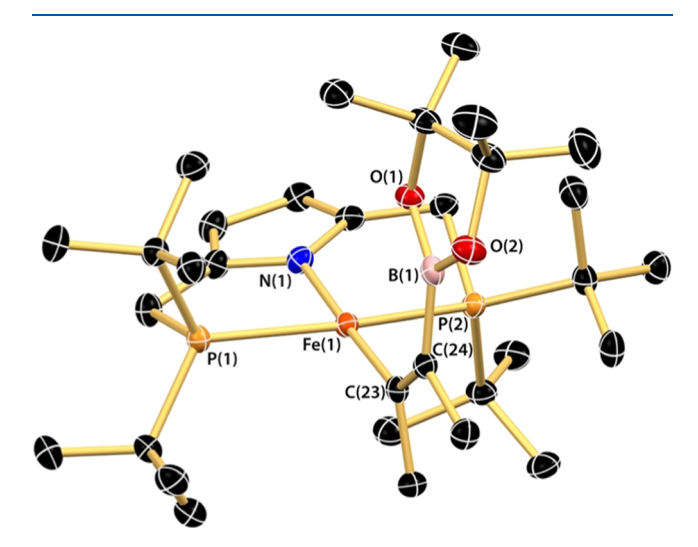


Figure 2. Solid-state structure of **5.** Hydrogen atoms are omitted for clarity. See the Supporting Information for bond distances and angles.

of the boryl complexes 1a and 1b and features a *cis* disposition of the methyl groups of the vinyl ligand, consistent with concerted insertion into the Fe–B bond. The Fe(1)-C(23) bond length of 1.962(2) Å is also considerably contracted from the value of 2.022(3) reported for $[Fe(Me)(^{tBu}PNP)]^{,27}$ in line with an sp² carbon center at C(23).

Following isolation of 5, we tested its reactivity with pinacolborane to determine if it is capable of generating a hydroborated product. Compound 5 did react with HBpin, albeit sluggishly, to generate the Z-diborated alkene (Scheme 3). Such a result requires concomitant formation of the hydride species, 2, which was also detected by NMR spectroscopy. In the presence of both HBpin and 2-butyne, 5 appeared to promote hydroboration. However, NMR analysis of these reactions indicated that consumption of 5 was minimal, and resonances attributable to a different ironvinyl species were also evident. The presence of this new ironvinyl species indicates the initial production of hydride 2 (vide infra). These results therefore demonstrate that catalytic reactions initiated by 1a are capable of producing hydroborated product, but this process most likely occurs through the initial reaction to generate a diborated product and complex 2.

Given the reactivity of 1a and alkyne, we next examined the analogous chemistry of 2 with 2-butyne. Upon addition of alkyne, 2 was consumed immediately to generate an initial iron species, which over time transformed into a second species when excess 2-butyne was present (Scheme 4). We have been

Scheme 4. Reactivity of Compound 2 with 2-Butyne

unable to isolate this initial species but propose that it is an iron-vinyl complex, 7, as expected for migratory insertion into the Fe-H bond. The ¹H NMR spectrum of this initial species shows a broadened resonance for the phosphine *tert*-butyl groups, consistent with hindered Fe-C rotation (see the Supporting Information). The second iron species observed in the presence of excess 2-butyne is most consistent with the double insertion product shown in Scheme 4. Its production occurs concomitantly with consumption of the initial iron species and only when excess 2-butyne is present. Moreover, the ¹H NMR spectrum of the second species shows additional resonances attributable to vinylic Me groups, further consistent with the structure proposed in Scheme 4.

In contrast to 5, addition of HBpin to a solution of in situgenerated 7 led to the rapid formation of the vinylboronate product (Scheme 4). Reaction of 7 with super-stoichiometric quantities of both 2-butyne and HBpin similarly produced the vinylboronate as the sole organic product but also displayed NMR resonances for both 5 and 7, with the latter predominating (ca. 95%, see the Supporting Information). Based on this reactivity, we propose that the vinyl intermediate 7 serves as the resting state during catalysis. Formation of 5 under these conditions likely occurs via side reactivity of 2 with HBpin (vide infra). During catalysis, this reactivity is likely minimal, provided that alkyne concentrations remain sufficiently high with respect to iron. Efforts to isolate 7 for further analysis have thus far been unsuccessful due to its reactive nature. We therefore targeted the related vinyl complex [Fe(CHCH₂)(tBuPNP)] (8) as a model for the key intermediate.

Synthesis of 8 was accomplished by addition of vinyl Grignard to $[FeCl(^{tBu}PNP)]$ in thf (Scheme 5). 1H NMR spectra of 8 display several paramagnetically shifted resonances akin to other S=1 species of $(^{tBu}PNP)Fe^{II}$. 31 Notably, the *tert*-butyl groups of 8 occur as a single resonance near -20 ppm, which is essentially identical to that observed for 7, further supporting the latter as a vinyl species. Crystallization of 8 from pentane afforded material suitable for X-ray diffraction, and the solid-state structure is depicted in Figure 3. The molecular geometry of 8 displays the expected square-planar

Scheme 5. Synthesis and Reactivity of 8

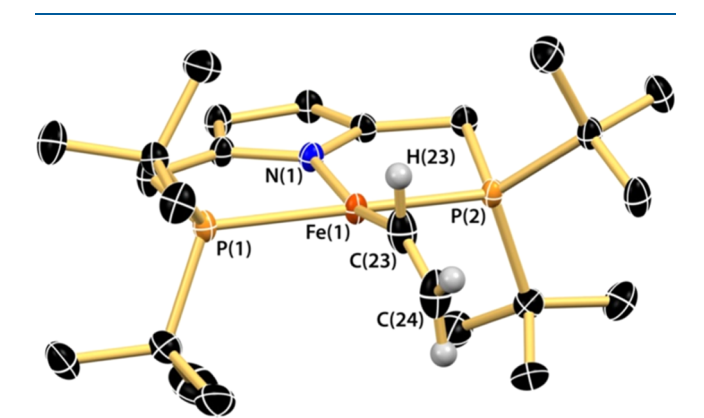


Figure 3. Thermal ellipsoid drawing (50%) of the solid-state structure of 8. Hydrogen atoms, with the exception of those bound to C(23) and C(24) are omitted for clarity. The position of H(23) was refined based on the electron density map. See the Supporting Information for bond distances and angles.

coordination observed for compounds **2** and **5**. Uniquely, however, the N(1)-Fe(1)-C(23) bond angle of **8** is significantly contracted from that of **5** (c.f. 166.5 vs 178.0°). Closer inspection of the structure also reveals a larger than expected Fe(1)-C(23)-C(24) angle of 142.8° and a shortened C(23)-C(24) distance of 1.30 Å. Each of these metrics is consistent with an α -agostic interaction in **8**. Refinement of the α -H atom position from the electron density map evinced an elongated C(23)-H(23) bond distance of 1.13 Å and a Fe(1)-H(23) contact of 2.51 Å, further consistent with an agostic interaction.

The stoichiometric reaction of 8 with HBpin resulted in the clean regeneration of 2 and the formation of H_2 CCHBpin (see the Supporting Information). However, the reaction was found to proceed far more sluggishly than that of 7, with only minimal conversion after several hours. We ascribe this slow reactivity to the aforementioned agostic interaction in 8, which likely serves to occlude access to the iron center.

Catalytic Reactions. Prior work with complexes 1a and 2 demonstrated their efficacy as catalysts for the hydroboration of several phenylacetylene derivatives under mild conditions. We therefore sought to extend this catalytic methodology to internal alkynes. Initial experiments focused on 2-butyne as a model substrate. Under all conditions examined, both 1a and 2 proved effective as precatalysts, producing the *E*-vinylboronate as the exclusive stereoisomer. Conversion was found to be essentially quantitative at room temperature in ca. 5 hours when employing 5 mol % of 1a (Table 1, entry 1). In comparison, reactions employing 2 under identical conditions

Table 1. Catalytic Hydroboration of 2-Butyne Employing 1a and 2 as Precatalysts^a

^aReaction conditions: Precatalyst **1a** or **2**, 2-butyne (80 mM), HBpin (88 mM), and 1,3,5-trimethoxybenzene (80 mM) as the internal standard in benzene- d_6 . ^bApproximate time required for >98% yield as determined by ¹H NMR integration.

required only 75 min to produce comparable yields (Table 1, entry 5). Heating the reaction mixtures to 68 °C permitted catalyst loadings as low as 0.25 mol % with completion in under 1 hour for both 1a and 2 (Table 1, entries 2–4 and 6–8). Results with these catalysts demonstrate that the (1Bu PNP)Fe system is not only efficient for the hydroboration of terminal alkynes but also for selected internal alkynes. In fact, hydroboration of 2-butyne proved more efficient than phenylacetylene, likely due to the influence of the aforementioned α -agostic interaction that should be present in alkyne insertion products of terminal acetylenes.

Comparing the results seen in entries 1 and 5 of Table 1, it is evident that precatalysts 1a and 2 operate with different activities for the hydroboration of 2-butyne. Given the stoichiometric results discussed above, we surmised that this difference was likely due to an induction period in the case of 1a, whereby 2 is generated during the initial stages of reaction and serves as the true catalyst. To test this hypothesis further, we examined the kinetic profile of catalytic reactions initiated by both 1a and 2 (Figure 4). Reactions employing precatalyst 1a demonstrated a lag period over the first 45 min. By contrast, reactions initiated with 2 displayed immediate hydroboration activity. These results further support a mechanism for hydroboration involving the iron-hydride, 2, as the key active species.

Additional kinetic experiments employing 2 were pursued to probe the reaction dependencies of the alkyne and hydroborane. Doubling the concentration of either 2-butyne or HBpin was found to produce a modest increase in the initial rate (see the Supporting Information). In neither case, however, was a clean doubling of the initial rate observed, suggesting a complex rate law with positive noninteger dependencies for both 2-butyne and HBpin. Given that we favor compound 7 as the resting state during catalysis, such rate information may reflect several of the off-cycle pathways discussed above (e.g., double alkyne insertion) that compete with productive hydroboration.

Given the positive results with 2-butyne, we next examined other internal alkynes to test whether the catalyst system would display comparable efficiency. Upon moving from 2-butyne to 4-octyne, we observed a slowing of the rate and a failure to reach completion at room temperature. Elevated

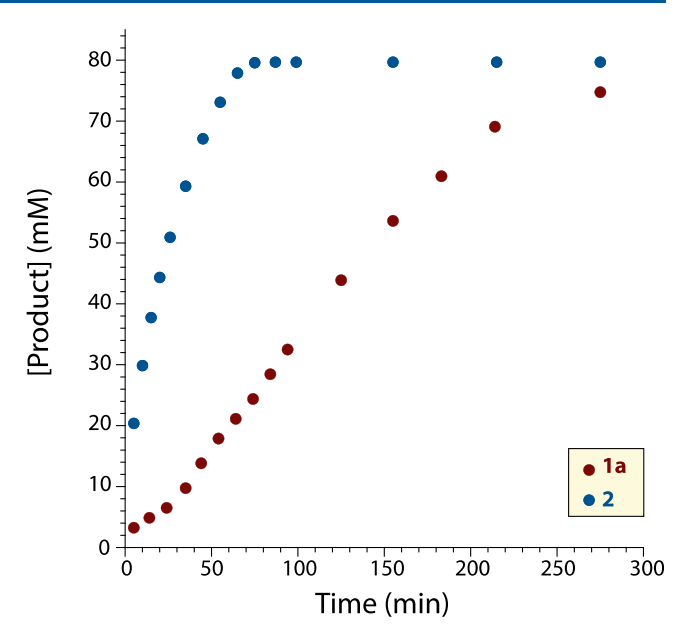


Figure 4. Reaction profile for hydroboration of 2-butyne by precatalysts **1a** and **2**. Reaction conditions are those of entries 1 and 5 in Table 1.

temperatures (68 °C) were necessary to reach full conversion, indicating that a direct reaction of **2** with HBpin and/or decomposition of the vinyl insertion product via β -H elimination may begin to outcompete insertion and hydroboration steps as the rate slows due to the large steric encumbrance of the alkyne substrate. Similar observations were found with diphenylacetylene in line with prior findings by Nishibayashi. In the case of diphenylacetylene, however, we detected hydrogenation of the alkyne as a significant byproduct. Stilbene, diborane, and H₂ were all detected by ¹H NMR spectroscopy throughout the course of the reaction, along with the desired hydroborated product. We explored the dynamics of the reaction by changing the ratio of substrate to reductant (Table 2). Increasing alkyne concentration was

Table 2. Catalytic Trials with 2 for the Hydroboration of Diphenylacetylene^a

"Reaction conditions: Precatalyst 2 (1 mol %), alkyne and borane equivalents as listed in table, 1,3,5-trimethoxybenzene (80 mM) as the internal standard in benzene- d_6 . Product ratio assayed by ¹H NMR spectroscopy after 24 h.

found to favor the formation of the hydrogenated product. This result is further consistent with a species akin to 7 serving as the resting state for hydroboration with diphenylacetylene. Reaction of the resulting alkyne insertion complex with HBpin is turnover-limiting, such that increasing alkyne concentration only leads to greater hydrogenation. Somewhat surprisingly, however, increasing the concentration of pinacolborane led to

no change in the product distribution. We ascribe this result to the ability of HBpin to undergo catalytic disproportionation in the presence of **2** when the reaction with the vinyl intermediate slows (*vide infra*).

The formation of stilbene during catalytic reactions of diphenylacetylene requires the presence of a hydrogen source. Catalytic disproportionation of HBpin could provide such a pathway while additionally accounting for the presence of $B_2 \mathrm{pin}_2$ in reactions of diphenylacetylene. To test this proposition, we examined the reactivity of HBpin with catalytic amounts of **2** in the absence of an alkyne. At room temperature, we found that formation of $B_2 \mathrm{pin}_2$ and H_2 gas occurs over 24 h (eq 1). The reaction proved slower than hydroboration of 2-butyne, although it likely becomes important with bulkier substrates such as diphenylacetylene. In such cases, it can also provide H_2 equivalents necessary for the observed hydrogenation reaction.

2HBpin
$$\xrightarrow{\text{5mol } \% 2}$$
 H₂ + B₂pin₂ (1)

As a final test of internal alkyne hydroboration, we probed the regioselectivity of the catalyst system by examining a nonsymmetric internal alkyne. In particular, we were curious to test whether 1a and 2 would yield different isomers. Accordingly, 1-phenyl-1-propyne was subjected to hydroboration by both precatalysts (Scheme 6). The two reactions

Scheme 6. Catalytic Hydroboration of 1-Phenyl-1-propyne with 1a and 2

were found to yield the same regioisomer, with the hydrogen atom ending up on the same carbon as the phenyl group (see the Supporting Information). These results further support a unified mechanism for both precatalysts 1a and 2. Moreover, the particular stereoisomer observed requires the insertion product featuring an α -methyl group (Scheme 6). Such a species much more closely resembles the intermediate formed during hydroboration of 2-butyne (7), accounting for the greater activity observed for 1-phenyl-1-propyne versus diphenylacetylene. Formation of the opposing insertion product with the phenyl group in the α position would be expected to lead to less efficient hydroboration due to the enhanced steric encumbrance near the metal center.

DISCUSSION

Based upon the experimental results described above, we favor the mechanistic cycle for alkyne hydroboration displayed in Scheme 7. When initiating catalysis with 1a (left part of the cycle), the alkyne can insert readily into the Fe-B bond to generate species such as 5 and 6. However, the resulting vinylic species react only slowly with the incoming HBpin to generate

the diborated alkene and 2. In addition, 1a can also react directly with pinacolborane to release B₂pin₂ and form 2 (eq 1), although this pathway is likely only operative when insertion of alkyne is very slow (e.g., with diphenylacetylene). In contrast to 1a, reactions initiated with 2 can insert alkyne to generate iron-vinyl intermediates such as 7 that react readily with HBpin to produce the product of hydroboration and regenerate the hydride.³³ As the steric bulk of the alkyne increases (4-octyne), the direct reaction of 2 with HBpin becomes more competitive, leading to the formation of 1a and partial catalyst deactivation. In the case of diphenylacetylene, the very sluggish reactivity of the vinyl intermediate leads to preferential disproportionation of HBpin by the (fBuPNP)Fe catalyst to form H_2 and the products of hydrogenation. We note that this catalytic mechanism explains many features of the observed system, including the diminished reactivity toward certain internal alkynes and the preferred regioselectivity in the case of unsymmetric and terminal acetylenes.

CONCLUSIONS

In summary, the mechanism of catalytic alkyne hydroboration has been scrutinized with both iron-hydride and iron-boryl species as precatalysts. Using 2-butyne as a model substrate, the data support the iron-hydride complex 2 as the true active species, with iron-vinyl compounds serving as the resting states during catalysis. By contrast, the iron-boryl compound was found to be chemically competent for hydroboration but only after an induction period, whereby it is transformed into the iron-hydride. This transformation can take place either through the reaction with alkyne and the formation of diborated product or through direct metathesis with HBpin to release B₂pin₂. Further support for a unified catalytic mechanism for both Fe-Bpin and Fe-H species was provided by the hydroboration of 1-phenyl-1-propyne, which resulted in the same regioisomer for both precatalysts. In the present system, the proclivity for alkyne insertion by both Fe-H and Fe-boryl species is notable and demonstrates the complexity of catalytic hydrofunctionalization reactions mediated by first-row metals, where several potential active species can demonstrate comparable reactivity. It is therefore advantageous, whenever possible, to interrogate the chemistry of such species in detail.

EXPERIMENTAL SECTION

General Comments. Manipulation of air- and moisture-sensitive materials was performed under an atmosphere of purified nitrogen gas using standard Schlenk techniques or in a Vacuum Atmospheres glovebox. Tetrahydrofuran, diethyl ether, pentane, and toluene were purified by sparging with argon and passing through two columns packed with 4 Å molecular sieves (all solvents) and alumina (THF and ether). 1,2-Dimethoxyethane (DME) and benzene- d_6 were dried over sodium ketyl and vacuum-distilled prior to use. 1 H NMR spectra were recorded in benzene- d_6 on Bruker spectrometers operating at 300 or 500 MHz (1 H) and referenced to the residual 1 H resonance of the solvent. Elemental analyses were performed by the CENTC facility at the University of Rochester. In each case, recrystallized material was used for the combustion analysis.

Materials. [FeH($^{\text{fBu}}$ PNP)] (2), [FeN $_2$ ($^{\text{fBu}}$ PNP)], and [FeCl($^{\text{fBu}}$ PNP)] were prepared according to published procedures or with slight modifications thereof. HBpin, B $_2$ pin $_2$, vinylmagnesium bromide, sodium borohydride (NaBH $_4$), 2-butyne, 4-octyne, diphenylacetylene, and 1-phenyl-1-propyne were purchased from commercial suppliers and used as received.

Crystallography. Crystals suitable for X-ray diffraction were mounted using Paratone oil onto a nylon loop. Data were collected at 98(2) K using a Rigaku AFC12/Saturn 724 CCD fitted with Mo K α

Scheme 7. Proposed Mechanism for Alkyne Hydroboration by 2

radiation (λ = 0.71075 Å) or at 100.0(1) K using a XtaLAB Synergy/Dualflex, HyPix fitted with Cu K α radiation (λ = 1.54184 Å). Data collection and unit cell refinement were performed using CrysAlisPro software.³⁴ Data processing and absorption correction were accomplished with CrysAlisPro and SCALE3 ABSPACK,³⁵ respectively. The structure, using Olex2,³⁶ was solved with the SHELXT structure solution program using direct methods and refined (on F^2) with the ShelXL refinement package³⁷ using full-matrix, least-squares techniques. All non-hydrogen atoms were refined with anisotropic displacement parameters. All hydrogen atom positions were determined by geometry and refined by a riding model.

[Fe(Bpin)(^{fBu}PNP)], 1a. Route 1. A flask was charged with 0.094 g (0.20 mmol) of [FeN₂(^{tBu}PNP)] and 8 mL of THF. Next, 0.205 g (0.80 mmol) of B₂pin₂ was added, and the mixture was allowed to stir overnight. The solvent was then removed under vacuum, and the residue was extracted into toluene and filtered through a pad of Celite. The filtrate was evaporated to dryness, leaving a dark yellow-brown residue. Treatment of the residue with pentane afforded 0.055 g (51%) of a yellow solid that was isolated by filtration. ¹H NMR data of the compound matched literature values.

Route 2. A flask was charged with 0.228 g (0.35 mmol) of Na[Fe(OPh)_2(^{\rm Bu}PNP)] (3) and 8 mL of THF. Next, 0.358 g (1.41 mmol) of bis(pinacolato) diboron (B_2pin_2) was added as a solid in one portion. The mixture was allowed to stir for 2 days, after which the solvent was removed under reduced pressure. The residue was extracted into toluene and filtered through a pad of Celite. The filtrate was evaporated to dryness affording a dark yellow-brown residue. The residue was washed with pentane, and the resulting solid was isolated by filtration to afford 0.145 g (73%) of the desired complex. Attempted crystallization from THF/pentane resulted in the precipitation of small amounts of dark solids, which were discarded. The remaining mother liquor was decanted and evaporated to dryness. Dissolution of the resulting residue in a saturated heptane solution at $-30\,^{\circ}\text{C}$ afforded yellow crystals of purified 1a. ^{1}H NMR data of the material matched literature values.

[Fe(Bcat)(^{tBu}**PNP)], 1b.** This compound was prepared on a small scale suitable for NMR and X-ray analysis in an identical fashion to **1a** from **3** and B₂cat₂. Crystals of **1b** suitable for X-ray diffraction were obtained from a saturated heptane solution at -30 °C. ¹H NMR (300 MHz): δ 22.17 (s, 2 cat-CH), 16.90 (s, 2 cat-CH), -11.11 (s, 2 pyr-CH), -14.62 (s, 36 *t*-Bu), -23.59 (s, 4 CH₂P).

Na[Fe(OPh)₂(^{tBu}PNP)], 3. A flask was charged with 0.176 g (0.37 mmol) of [FeCl(^{tBu}PNP)], 0.095 g (0.82 mmol) of sodium phenoxide, and 8 mL of THF. The solution was allowed to stir overnight at room temperature. The solvent was removed under

reduced pressure, leaving a dark brown residue that was then extracted into toluene. The toluene extract was filtered through a pad of Celite and transferred to a tared vial. The solvent was then evaporated to dryness, affording 0.176 g (73%) of crude product as an oily solid, which was employed for the synthesis of 1a without further purification. Crystals suitable for X-ray diffraction were grown by vapor diffusion of pentane into THF at $-30\,^{\circ}\mathrm{C}$. ¹H NMR spectra of 3 were essentially featureless, with the exception of a large, broad resonance centered at -24.7 ppm in benzene- d_6 .

[Fe(BH₄)(^{tBu}PNP)], **4.** A scintillation vial was charged with 0.141 g (0.30 mmol) of [FeCl(^{tBu}PNP)], 0.012 g of NaBH₄ (0.33 mmol), and 5 mL of DME. The mixture was allowed to stir overnight at room temperature. The solvent was removed under reduced pressure, leaving a dark orange residue that was then extracted into toluene. The toluene extract was filtered through a pad of Celite and evaporated to dryness. The remaining dark orange solid was washed with pentane and isolated by filtration to afford 0.118 g (87%). Crystals suitable for X-ray diffraction were grown from a saturated diethyl ether solution at -30 °C. ¹H NMR (300 MHz): $\delta - 16.70$ (s, 4 CH₂P), -20.80 (s, 36 t-Bu), -25.55 (s, 2 pyr-CH). Anal. Calcd for C₂₂H₄₆BFeNP₂: C, 58.30; H, 10.23; N, 3.09. Found: C, 57.68; H, 10.30; N, 2.99.

[Fe(C{Me}C{Me}Bpin)(^{tBu}PNP)], **5.** A flask was charged with 0.069 g (0.12 mmol) of **1a** and 5 mL of THF. The bright yellow solution darkened slightly upon addition of 14.3 μ L of 2-butyne (0.18 mmol). The resulting solution was allowed to stir overnight at room temperature, after which the solvent was removed under reduced pressure. The remaining brown residue was washed with pentane and isolated by filtration to afford 0.0564 g (75%) of a brown solid. Crystals suitable for X-ray diffraction were grown from a saturated diethyl ether solution at $-30\,^{\circ}$ C. 1 H NMR (300 MHz): δ -1.62 (s, 3 viny-Me), -4.88 (s, 12 Bpin), -5.85 (s, 2 pyr-CH), -13.49 (br s, 2 CH₂P), -14.57 (br s, 18 t-Bu), -16.70 (br s, 18 t-Bu), -37.18 (br s, 2 CH₂P). Anal. Calcd for C₃₂H₆₀BFeNO₂P₂: C, 62.05; H, 9.76; N, 2.26. Found: C, 59.10; H, 9.83; N, 1.30. Repeated analyses returned low values for C, H, and N, likely due to decomposition.

[Fe(C{Pr}C{Pr}Bpin)($^{\text{tBu}}$ PNP)], **6.** A flask was charged with 0.0652 g (0.12 mmol) of **1a** and 5 mL of THF. To the stirring solution was added 18.6 μL (0.13 mmol) of 4-octyne. Upon addition, the color remained bright yellow. The mixture was allowed to stir overnight, after which all volatiles were removed in vacuo. The oily yellow residue was then extracted into toluene, filtered through a pad of Celite, and transferred to a tared vial. The solvent was then evaporated to dryness, affording 0.051 g (66%) of a gummy solid. ¹H NMR (300 MHz): δ 68.40 (br s, 2 CH₂), 35.82 (br s, 2 CH₂),

26.44 (br s, 2 CH_2), 24.15 (s, 3 CH_2CH_3), 19.11 (br s, 3 CH_2CH_3), 2.0 (br s, 12 Bpin), -19.47 (br s, 18 t-Bu + 2 $CH_2P + 2$ pyr-CH), -23.16 (s, 18 t-Bu), -24.7 (br s, 2 CH_2P).

[Fe(CHCH₂)(t^{Bu}PNP)], **8.** A flask was charged with 0.0754 g (0.16 mmol) of [FeCl(t^{Bu}PNP)] and 5 mL of THF. To the mixture was added 0.25 mL (0.18 mmol) of 0.70 M solution of vinylmagnesium bromide in THF. Upon addition, the color changed from dark orange to a light tan color. The mixture was allowed to stir overnight. Next, 1,4-dioxane was added to the mixture and left to stir for 5 min, after which all volatiles were removed in vacuo. The brown residue was then extracted into toluene and filtered through a pad of Celite and evaporated to dryness. The remaining solid was washed with pentane and isolated by filtration to afford 0.0622 g (84%) of a brown solid. Crystals suitable for X-ray diffraction were grown from a saturated diethyl ether solution at -30 °C. ¹H NMR (300 MHz, δ): 100.1 (br s, 1 vinyl-CH), -11.26 (s, 2 pyr-CH), -17.79 (s, 4 CH₂P), -18.51 (s, 36 t-Bu), -73.64 (s, 1 vinyl-CH). Anal. Calcd for C₂₄H₄₅FeNP₂: C, 61.94; H, 9.75; N, 3.01. Found: C, 62.18; H, 9.76; N, 2.82.

General Procedure for Catalytic Hydroboration. An NMR tube was charged with 2-butyne (0.032 mmol) or other alkynes, HBpin (0.035 mmol), and 1,3,5-trimethoxybenzene (0.032 mmol) as an internal standard. The contents of the tube were dissolved in 400 μ L of benzene- d_6 . Precatalyst 1a or 2 was then added as a 10 mM stock solution in benzene- d_6 to give the desired catalyst loading. The NMR tube was shaken and rapidly transferred to the spectrometer. The course of the reaction was followed via ¹H NMR spectroscopy. For reactions performed at elevated temperature, the NMR tube was immersed in an oil bath between data acquisitions.

Procedure for the Catalytic Disproportionation of HBpin by 2. An NMR tube was charged with HBpin (0.014 mmol) and 1,3,5-trimethoxybenzene (0.015 mmol) as an internal standard. The contents of the tube were dissolved in 400 μ L of benzene- d_6 . Catalyst 2 (0.67 μ mol, ca. 5 mol %) was then added as a 10 mM solution in benzene- d_6 . The NMR tube was shaken and rapidly transferred to the spectrometer. The course of the reaction was followed by 1 H NMR spectroscopy; formation of H_2 and $B_2 pin_2$ was observed over time as the sole products.

ASSOCIATED CONTENT

5 Supporting Information

The Supporting Information is available free of charge at https://pubs.acs.org/doi/10.1021/acs.inorgchem.2c01325.

¹H NMR spectra of all compounds and select reactions, additional thermal ellipsoid drawings, and tables of crystallographic refinement parameters (PDF)

Accession Codes

CCDC 2161460-2161464 contain the supplementary crystallographic data for this paper. These data can be obtained free of charge via www.ccdc.cam.ac.uk/data_request/cif, or by emailing data_request@ccdc.cam.ac.uk, or by contacting The Cambridge Crystallographic Data Centre, 12 Union Road, Cambridge CB2 1EZ, UK; fax: +44 1223 336033.

AUTHOR INFORMATION

Corresponding Author

Zachary J. Tonzetich — Department of Chemistry, University of Texas at San Antonio (UTSA), San Antonio, Texas 78249, United States; orcid.org/0000-0001-7010-8007; Email: zachary.tonzetich@utsa.edu

Authors

Ana L. Narro – Department of Chemistry, University of Texas at San Antonio (UTSA), San Antonio, Texas 78249, United States Hadi D. Arman – Department of Chemistry, University of Texas at San Antonio (UTSA), San Antonio, Texas 78249, United States

Complete contact information is available at: https://pubs.acs.org/10.1021/acs.inorgchem.2c01325

Author Contributions

The manuscript was written through contributions of all authors. All authors have given approval to the final version of the manuscript.

Notes

The authors declare no competing financial interest.

ACKNOWLEDGMENTS

The authors thank the Welch Foundation (AX-1772) for financial support of this work. Dr. Daniel Wherritt is acknowledged for assistance in acquiring and analyzing HMBC data. NMR and X-ray facilities at UTSA were acquired with support from the National Science Foundation (CHE-1625963 and CHE-1920057).

REFERENCES

- (1) Brown, H. C. Organic Synthesis via Boranes. Wiley-Interscience: New York, 1975.
- (2) Beletskaya, I.; Pelter, A. Hydroborations catalysed by transition metal complexes. *Tetrahedron* **1997**, *53*, 4957–5026.
- (3) Gunanathan, C.; Hölscher, M.; Pan, F.; Leitner, W. Ruthenium Catalyzed Hydroboration of Terminal Alkynes to Z-Vinylboronates. *J. Am. Chem. Soc.* **2012**, *134*, 14349–14352.
- (4) Bose, S. K.; Mao, L.; Kuehn, L.; Radius, U.; Nekvinda, J.; Santos, W. L.; Westcott, S. A.; Steel, P. G.; Marder, T. B. First-Row d-Block Element-Catalyzed Carbon-Boron Bond Formation and Related Processes. *Chem. Rev.* **2021**, *121*, 13238–13341.
- (5) Merz, L. S.; Ballmann, J.; Gade, L. H. Phosphines and N-Heterocycles Joining Forces: an Emerging Structural Motif in PNP-Pincer Chemistry. *Eur. J. Inorg. Chem.* **2020**, 2020, 2023–2042.
- (6) Peris, E.; Crabtree, R. H. Key factors in pincer ligand design. Chem. Soc. Rev. 2018, 47, 1959–1968.
- (7) Dahlhoff, W. V.; Nelson, S. M. Studies on the magnetic cross-over in five-co-ordinate complexes of iron(II), cobalt(II), and nickel(II). Part II. *J. Chem. Soc. A* **1971**, 2184–2190.
- (8) Arevalo, R.; Chirik, P. J. Enabling Two-Electron Pathways with Iron and Cobalt: From Ligand Design to Catalytic Applications. *J. Am. Chem. Soc.* **2019**, *141*, 9106–9123.
- (9) Wei, D.; Darcel, C. Iron Catalysis in Reduction and Hydrometalation Reactions. *Chem. Rev.* **2019**, *119*, 2550–2610.
- (10) Garhwal, S.; Fridman, N.; de Ruiter, G. Z-Selective Alkyne Functionalization Catalyzed by a trans-Dihydride N-Heterocyclic Carbene (NHC) Iron Complex. *Inorg. Chem.* **2020**, *59*, 13817–13821.
- (11) Obligacion, J. V.; Chirik, P. J. Earth-abundant transition metal catalysts for alkene hydrosilylation and hydroboration. *Nat. Rev. Chem.* **2018**, *2*, 15–34.
- (12) Chen, J.; Xi, T.; Lu, Z. Iminopyridine Oxazoline Iron Catalyst for Asymmetric Hydroboration of 1,1-Disubtituted Aryl Alkenes. *Org. Lett.* **2014**, *16*, 6452–6455.
- (13) Zhang, F.; Song, H.; Zhuang, X.; Tung, C.-H.; Wang, W. Iron-Catalyzed 1,2-Selective Hydroboration of N-Heteroarenes. *J. Am. Chem. Soc.* **2017**, *139*, 17775–17778.
- (14) Das, U. K.; Higman, C. S.; Gabidullin, B.; Hein, J. E.; Baker, R. T. Efficient and Selective Iron-Complex-Catalyzed Hydroboration of Aldehydes. *ACS Catal.* **2018**, *8*, 1076–1081.
- (15) Bai, T.; Janes, T.; Song, D. Homoleptic iron(ii) and cobalt(ii) bis(phosphoranimide) complexes for the selective hydrofunctionalization of unsaturated molecules. *Dalton Trans.* **2017**, *46*, 12408–12412.

- (16) Chen, C.; Shen, X.; Chen, J.; Hong, X.; Lu, Z. Iron-Catalyzed Hydroboration of Vinylcyclopropanes. *Org. Lett.* **2017**, *19*, 5422–5425.
- (17) Haberberger, M.; Enthaler, S. Straightforward Iron-Catalyzed Synthesis of Vinylboronates by the Hydroboration of Alkynes. *Chem.-Asian J.* **2013**, *8*, 50–54.
- (18) MacNair, A. J.; Millet, C. R. P.; Nichol, G. S.; Ironmonger, A.; Thomas, S. P. Markovnikov-Selective, Activator-Free Iron-Catalyzed Vinylarene Hydroboration. ACS Catal. 2016, 6, 7217–7221.
- (19) Ogawa, T.; Ruddy, A. J.; Sydora, O. L.; Stradiotto, M.; Turculet, L. Cobalt- and Iron-Catalyzed Isomerization—Hydroboration of Branched Alkenes: Terminal Hydroboration with Pinacolborane and 1,3,2-Diazaborolanes. *Organometallics* **2017**, *36*, 417–423
- (20) Tseng, K.-N. T.; Kampf, J. W.; Szymczak, N. K. Regulation of Iron-Catalyzed Olefin Hydroboration by Ligand Modifications at a Remote Site. *ACS Catal.* **2015**, *5*, 411–415.
- (21) Greenhalgh, M. D.; Thomas, S. P. Chemo-, regio-, and stereoselective iron-catalysed hydroboration of alkenes and alkynes. *Chem. Commun.* **2013**, *49*, 11230–11232.
- (22) Gorgas, N.; Alves, L. G.; Stöger, B.; Martins, A. M.; Veiros, L. F.; Kirchner, K. Stable, Yet Highly Reactive Nonclassical Iron(II) Polyhydride Pincer Complexes: Z-Selective Dimerization and Hydroboration of Terminal Alkynes. *J. Am. Chem. Soc.* **2017**, *139*, 8130–8133.
- (23) Gorgas, N.; Stöger, B.; Veiros, L. F.; Kirchner, K. Iron(II) Bis(acetylide) Complexes as Key Intermediates in the Catalytic Hydrofunctionalization of Terminal Alkynes. *ACS Catal.* **2018**, 8, 7973–7982.
- (24) Espinal-Viguri, M.; Woof, C. R.; Webster, R. L. Iron-Catalyzed Hydroboration: Unlocking Reactivity through Ligand Modulation. *Chem.-Eur. J.* **2016**, 22, 11605–11608.
- (25) Nakajima, K.; Kato, T.; Nishibayashi, Y. Hydroboration of Alkynes Catalyzed by Pyrrolide-Based PNP Pincer—Iron Complexes. *Org. Lett.* **2017**, *19*, 4323–4326.
- (26) Thompson, C. V.; Arman, H. D.; Tonzetich, Z. J. Investigation of Iron Silyl Complexes as Active Species in the Catalytic Hydrosilylation of Aldehydes and Ketones. *Organometallics* **2022**, *41*, 430–440.
- (27) Kuriyama, S.; Arashiba, K.; Nakajima, K.; Matsuo, Y.; Tanaka, H.; Ishii, K.; Yoshizawa, K.; Nishibayashi, Y. Catalytic transformation of dinitrogen into ammonia and hydrazine by iron-dinitrogen complexes bearing pincer ligand. *Nat. Commun.* **2016**, *7*, 12181.
- (28) Tran, B. L.; Adhikari, D.; Fan, H.; Pink, M.; Mindiola, D. J. Facile entry to 3d late transition metal boryl complexes. *Dalton Trans.* **2010**, *39*, 358–360.
- (29) Thompson, C. V.; Davis, I.; DeGayner, J. A.; Arman, H. D.; Tonzetich, Z. J. Iron Pincer Complexes Incorporating Bipyridine: A Strategy for Stabilization of Reactive Species. *Organometallics* **2017**, 36, 4928–4935.
- (30) Krishnan, V. M.; Arman, H. D.; Tonzetich, Z. J. Preparation and reactivity of a square-planar PNP cobalt(II)—hydrido complex: isolation of the first {Co-NO}⁸—hydride. *Dalton Trans.* **2018**, 47, 1435—1441.
- (31) Thompson, C. V.; Tonzetich, Z. J. Pincer Ligands Incorporating Pyrrolyl Units: Versatile Platforms for Organometallic Chemistry and Catalysis. In *Advances in Organometallic Chemistry*, Pérez, P. J., Ed.; 2020; Vol. 74, Chapter 4, pp 153–240.
- (32) Brookhart, M.; Green Malcolm, L. H.; Parkin, G. Agostic interactions in transition metal compounds. *Proc. Natl. Acad. Sci. U.S.A.* **2007**, *104*, 6908–6914.
- (33) Blasius, C. K.; Vasilenko, V.; Matveeva, R.; Wadepohl, H.; Gade, L. H. Reaction Pathways and Redox States in α -Selective Cobalt-Catalyzed Hydroborations of Alkynes. *Angew. Chem., Int. Ed.* **2020**, 59, 23010–23014.
- (34) CrysAlisPro, Rigaku Oxford Diffraction: Rigaku Corporation, The Woodlands, TX, 2015.
- (35) SCALE3 ABSPACK—An Oxford Diffraction Program, Oxford Diffraction Ltd., 2005.

- (36) Dolomanov, O. V.; Bourhis, L. J.; Gildea, R. J.; Howard, J. A. K.; Puschmann, H. OLEX2: a complete structure solution, refinement and analysis program. *J. Appl. Crystallogr.* **2009**, *42*, 339–341.
- (37) Sheldrick, G. M. A short history of SHELX. *Acta Crystallogr. A* **2008**, *64*, 112–122.